International Journal of Heat and Mass Transfer 94 (2016) 20–28

Contents lists available at ScienceDirect

International Journal of Heat and Mass Transfer

journal homepage: www.elsevier.com/locate/ijhmt

Thermal conductivity enhancement of platelets aligned composites with volume fraction from 10% to 20%

Chao Yuan, Bin Xie, Mengyu Huang, Ruikang Wu, Xiaobing Luo *

State Key Laboratory of Coal Combustion, School of Energy and Power Engineering, Huazhong University of Science and Technology, Wuhan 430074, China

ARTICLE INFO

Article history:
Received 6 October 2015
Received in revised form 13 November 2015
Accepted 17 November 2015

Keywords:
Thermal conductivity
Hexagonal boron nitride
Polymer composites
Magnetic alignment
Mechanical vibration

ABSTRACT

Hexagonal boron nitride (hBN)-filled composites are widely used in electronics for thermal management. In order to enhance the materials heat transport capability, the hBN platelets are expected to be assembled into well-ordered structure. Such structure has been achieved in practice by the magnetic alignment approach. However, this approach is limited to the composites loaded with low volume fraction of platelets (<10%). In this paper, we report the use of combined mechanical and magnetic stimuli to fabricate the well-aligned composites at the volume fraction from 10% to 20%. The platelets in the resulting composites exhibit a high degree of alignment. For instance, in the 10 vol.% composite, the angle of 95.3% of platelets is greater than 45°, only ~5% of platelets falls into the horizontal direction. Thermal conductivity of the composites was investigated experimentally. It exhibited strong correlation with the platelets alignment. The measured thermal conductivity of 10 vol.% aligned composite is 74% higher than that of unaligned composite. Thermal conductivity were also analyzed by a theoretical model. Thermal boundary resistance (R_b), arising at the platelets–matrix interface, was extracted by fitting the measured thermal conductivity to model prediction. R_b is found to decrease with the increase of alignment degree. This study suggests that assembling the platelets into well-ordered structure can greatly enhance the heat transport capability due to the formation of conductive networks and the reduction of R_b.

1. Introduction

Excellent electrically insulating and thermally conductive properties have made polymer-based composites widely used in electronics for thermal management [1–4]. The polymeric composites are predominantly assembled with highly thermally conductive fillers, such as ceramics, metals or metal oxides [5–9]. Among various particles, hexagonal boron nitride (hBN) has been frequently chosen as the reinforcing filler. As schematically shown in Fig. 1a, hBN is a platelet-shaped, high aspect ratio (D/t) particle and possesses high in-plane thermal conductivity (~390 W m^{-1} K^{-1}) [10]. In most thermal management applications, as shown in Fig. 1b, the hBN-filled composite is expected to provide efficient heat flow (Q) from the heat source to heat sink in the direction normal to the composite layer. So the ideal orientation of hBN platelets in polymeric matrix is parallel to the direction of Q (Fig. 1b (I)). Such well-ordered structures can make the composite take full advantage of platelets high in-plane thermal conductivity. On the contrary, the isotropic (Fig. 1b (II)) orientation is much less favorable. Therefore, control of the platelets orientation can enable the enhancement of composites heat transport capability.

The well-ordered structures has been achieved in practice by several approaches, including tape-cast [11], spin-cast [12], shear alignment [13], electrical alignment [14], and magnetic alignment [15–17]. Among these approaches, magnetic alignment has been recently highlighted due to the remote control of fillers orientation and possibility of aligning fillers at arbitrary directions [17,18]. This approach relies on coating the hBN platelets with magnetic nanoparticles, such as Ni, Fe, Co [16] and Fe_3O_4 [15,17]. These modified hBN (mhBN) platelets exhibit a high magnetic response which enables the alignment of them in low-viscosity suspending fluids under linear, uniform magnetic field [15–17]. Then the magnetically-imposed alignment can be fixed by consolidating the suspending fluids.

However, this approach is limited to the composites loaded with low volume fraction (f) of mhBN platelets. When f increases above a percolation threshold, the steric interactions between the platelets will dominate, which hinders the platelets alignment. For instance, applying such approach, Lin et al. [17] prepared the aligned composites at f from 3% to 28%. When f was below 13%, the platelets could be assembled into highly ordered structures in composites. While, as f increases above 13%, significant amount

* Corresponding author.
E-mail address: luoxb@hust.edu.cn (X. Luo).

http://dx.doi.org/10.1016/j.ijheatmasstransfer.2015.11.045
0017-9310/

Nomenclature

C_p	heat capacity, J kg^{-1} K^{-1}
D	diameter of platelet, μm
d	diameter of iron oxide nanoparticles, μm
f	platelet volume fraction, %
H_0	intensity of the magnetic field, Gs
I	peak intensity of X-ray diffraction
k^*_{33}	effective through-plane thermal conductivity of composites, W m^{-1} K^{-1}
k^c_{ii}	equivalent thermal conductivity along the ii symmetric axis of the composite unit cell, W m^{-1} K^{-1}
k_m	thermal conductivity of matrix, W m^{-1} K^{-1}
k_p	thermal conductivity of platelet, W m^{-1} K^{-1}
k_T	measured through-plane thermal conductivity of composites, W m^{-1} K^{-1}
L_{ii}	geometrical factor
P	population-fraction of the platelets to be above 45°, %
p	inverse of particle aspect ratio
Q	heat flow, W m^{-2}
R_b	thermal boundary resistance at the platelet–matrix interface, m^2 W K^{-1}
t	thickness of platelet, nm
w	rotating frequency, Hz
w_c	critical frequency, Hz

Greek symbols

α	thermal diffusivity, m^2 s^{-1}
μ_0	magnetic permeability of free space, m kg s^{-2} A^{-2}
θ	angle between the composite axis and the local particle symmetric axis, degree
ρ	density, kg m^{-3}
$\rho(\theta)$	distribution function describing the orientation of particles
η	viscosity of matrix, Pa s
χ_{ps}	magnetic susceptibility of the platelet shell

Subscripts

002	peaks of horizontally oriented hexagonal boron nitride
100	peaks of vertically oriented hexagonal boron nitride
11	in-plane direction
33	through-plane direction

of unaligned mhBN platelets were found in composites. In addition, in our previous [15] and Boussaad [16] work, the examples of well-aligned composites obtained by this approach have a maximum f of 9.14% and 10%, respectively.

To overcome the strong steric hindrances between platelets and thus achieve high degree of alignment, one possible method is to provide additional energy to platelets during magnetic alignment. Mechanical vibration is such a candidate as the additional energy, which is often applied for the arrangement of disordered particles [19–21]. Furthermore, the former investigation [22] has shown the possibility in assembling the high concentrations of alumina platelets into ordered architectures using magnetic fields and mechanical vibration. The results show that the mechanical properties of the alumina-reinforced composites can be tuned deliberately. Therefore, it is possible to tailor the thermal property of the platelets-reinforced composites with such strategy.

In this work, we investigated the thermal conductivity of polymer-based composites containing high concentrations of aligned hBN platelets. The outline of this work is as follows. In the beginning, the aligned composites were fabricated using combined mechanical and magnetic stimuli. For the purpose of comparison, the composites were also prepared with the former magnetic approach [15,17]. Then, the cross section of those composites was imaged by scanning electron microscopy (SEM) and the degree of platelets alignment were quantitatively examined by measuring the platelets angles (θ) with the SEM images. After that, X-ray diffraction (XRD) analysis was carried out to further evaluate the degree of alignment. Finally, thermal conductivities of those composites were compared and analyzed in light of platelets alignment degree.

2. Experimental section

2.1. Materials

hBN platelets (AC6041), with an averaged diameter (D) of 5 μm, were purchased from Momentive. The thickness (t) of platelets is estimated to be 250 nm [17], leading to an average D/t of 20. Epoxy resin, supplied by Huntsman, was selected as the polymer matrix. It composes of a low viscosity bisphenol-A based liquid resin (Araldite LY1564) and an amine based hardener (Aradur 3487). The mix ratio is 100:34 by weight. The initial viscosity (η) of the mixture is about 0.27 Pa s at 25 °C. The aqueous-based EMG-605 ferrofluid used to magnetize the hBN platelets was kindly supplied by Ferrotec. It contained 3.9 vol.% iron oxide nanoparticles coated with a cationic surfactant. The average diameter (d) of nanoparticles is 20 nm [15].

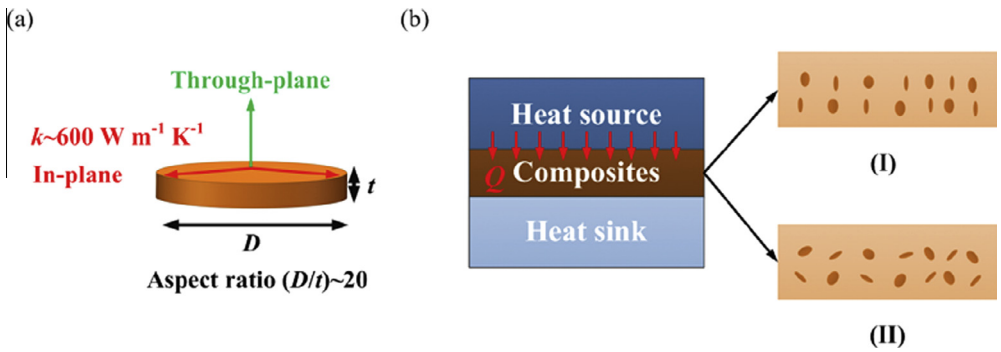

Fig. 1. (a) Representation of hBN platelet geometry and thermal property. (b) Schematic showing the utilization of hBN-filled composite for the heat dissipation from heat source to heat sink. Orientations of hBN platelets in the composite layer: (I) through-plane and (II) isotropic.

2.2. Preparation of magnetically responsive hBN (mhBN) platelets

hBN platelets were coated with superparamagnetic iron oxide nanoparticles to make them magnetized via a previously reported method [15,17–18]. Specifically, 4 g of hBN platelets were dispersed in 200 mL of deionized water at pH = 7, while 400 μL of ferrofluid diluted in 5 ml of deionized water was added dropwise. In the deionized water, the hBN platelets have a negative surface charge, causing the positively charged magnetic nanoparticles to electrostatically adsorb on the hBN surface. The adsorption was considered complete when the supernatant was clear. After that, the coated platelets were rinsed three times with deionized water. Finally, the magnetized platelets were dried in an oven at 90 °C for 12 h. The SEM image (Fig. 4d) provided by our previous work [15] has shown the nanostructure of the obtained platelet, which confirmed the successful attachment of iron oxide nanoparticles to the platelet surface.

2.3. Preparation of composites with aligned mhBN platelets

Composites were prepared using the epoxy resin and mhBN platelets. mhBN platelets was first suspended in the mixture of Araldite LY1564 resin and Aradur 3487 hardener. The resulting suspension was mechanically stirred for 10 min to be fully dispersed. Next, the suspension was sent into vacuum chamber to remove the bubbles introduced during the mixing step. After that, the polymer suspension was cast into a 10 mm × 10 mm × 2 mm Teflon mold.

Fig. 2a schematically shows the way of aligning mhBN platelets in matrix. The Teflon mold containing the suspension was fixed with a vibrating table and placed under a 40 mm × 40 mm × 20 mm rare earth magnet which was connected to a motor. The table could provide the continuous mechanical vibration to the sample with a power of 550 W and an amplitude of 0.5 mm. The magnet, rotated with a fixed frequency (w), produced a rotating magnetic field of about 8000 Gs in the plane normal to the suspension. According to Ref. [23], in order to achieve the vertical alignment of platelets, w should be larger than a critical frequency (w_c). In this study, w_c is calculated to be about 0.3 Hz (see details in Appendix A), and then w is set to be 5 Hz. The mechanical vibration last for 30 min. Then, the sample was kept in the rotating magnetic field for 6 h to form the ordered structures. Afterwards, the sample was placed into an oven at 60 °C for 4 h. During this period, the sample was still exposed to a linear, uniform, vertical magnetic field to keep the obtained structures. The vertical magnetic field was produced by two parallel arranged 200 mm × 100 mm custom rectangular magnets. Finally, an annealing step at 120 °C for 2 h was conducted to ensure the full curing of the sample.

For comparison, the composites were also prepared with the former magnetic approach [15,17]. Fig. 2b depicts the process of fabrication. Firstly, the Teflon mold containing the suspension was positioned in the uniform, vertical magnetic field for 4 h at 25 °C. Afterwards, the sample was heated with the magnetic field at 60 °C for 4 h and 120 °C for 2 h.

The composites were also fabricated without any stimuli to obtain the unaligned composites. Fig. 2c schematically shows the process of fabrication. In the beginning, the Teflon mold containing the suspension was incubated for 4 h at 25 °C. Then, the sample was placed in the oven at 60 °C for 4 h and 120 °C for 2 h.

2.4. Characterization of mhBN–resin composites

The morphology of mhBN platelets was observed by imaging the polished surfaces of samples using a scanning electron microscopy (SEM, Quanta 200) at an accelerating voltage of 20 kV. To get the polished surfaces, samples embedded into epoxy resin was ground with silicon carbide foils (grits: 600, 1200, 1500 and 2000) and polished with diamond suspension (grain size: 7 μm, 3 μm and 1.5 μm). Before visualization, the polished surfaces were sputtered with a thin layer of gold for better imaging. The angle distributions of mhBN platelets were analyzed with ImageJ (NIH).

X-ray diffraction (XRD) analysis of mhBN–resin composites was also conducted to evaluate the orientation of mhBN platelets in composites. This analysis was carried out with D/MAX-RB using Cu Kα radiation (40 kV and 40 mA). Before the tests, the samples were ground with silicon carbide foils (600, 1500 and 2000) to expose the inner surfaces.

2.5. Evaluation of composites thermal conductivity

Thermal conductivity was calculated according to the formula:

$$k = \alpha C_p \rho \quad (1)$$

where C_p, ρ and α are heat capacity, density and thermal diffusivity of sample, respectively. C_p was measured by a differential scanning calorimetry (Diamond DSC, PerkinElmer Instruments). ρ was calculated according to sample weight and dimensions. α was measured by a laser flash apparatus (LFA457, Netzsch) at 25 °C. Before the test, the sample surfaces were coated with a thin graphite film to increase the energy absorption and the emittance of the surfaces. In the test, heat propagates from the bottom to the top surface of sample.

3. Results and discussion

3.1. Characterization of the composites

In this study, the resin-based composites, prepared with combined mechanical and magnetic stimuli, uniform magnetic stimuli and no stimuli, are named as MM-mhBN–resin, M-mhBN–resin and R-mhBN–resin, respectively. Fig. 3a illustrates the ideal microstructure of the aligned composites. In the three-dimensional (3D) view, all platelets orient to the vertical orientation. In the cross section view, the platelets are projected as two representative morphologies: 1D vertical rods and 2D plates, which are indicated by green and blue arrows, respectively. Cross-sectional SEM images of 10 vol.% mhBN–resin composites are shown in Fig. 4a–c. Fig. 4a shows that, in MM-mhBN–resin, a large number of platelets are projected as the two representative morphologies. Few platelets orient to the horizontal direction. In contrast, in the cross sectional view of M-mhBN–resin (Fig. 4b), although the majority of platelets are aligned along the vertical direction, a number of platelets, indicated by red arrows, orient to the horizontal direction. Fig. 4c gives the cross sectional view of R-mhBN–resin. Both vertical and horizontal alignment characterizations can be easily found in the SEM image.

Parts d and g of Fig. 4 show the cross-sectional SEM images of 15 vol.% and 20 vol.% MM-mhBN–resin composites. Quantities of platelets are projected as the representative morphologies. However, with the increase of platelets loading, some unexpected platelets, which orient to the horizontal direction, are observed in the MM-mhBN–resin. Parts (e, h) and (f, i) of Fig. 4 give the cross-sectional views of M-mhBN–resin and R-mhBN–resin composites, respectively. In M-mhBN–resin, the horizontally oriented platelets also increase with the increase of loading. In R-mhBN–resin, both vertically and horizontally oriented mhBN platelets can be found abundantly. So we assume that mhBN platelets orient randomly in R-mhBN–resin composites.

We quantitatively examine the degree of platelets alignment by measuring the platelets angles (θ) with the SEM images. As schematically shown in Fig. 3b, θ is angle between the composite

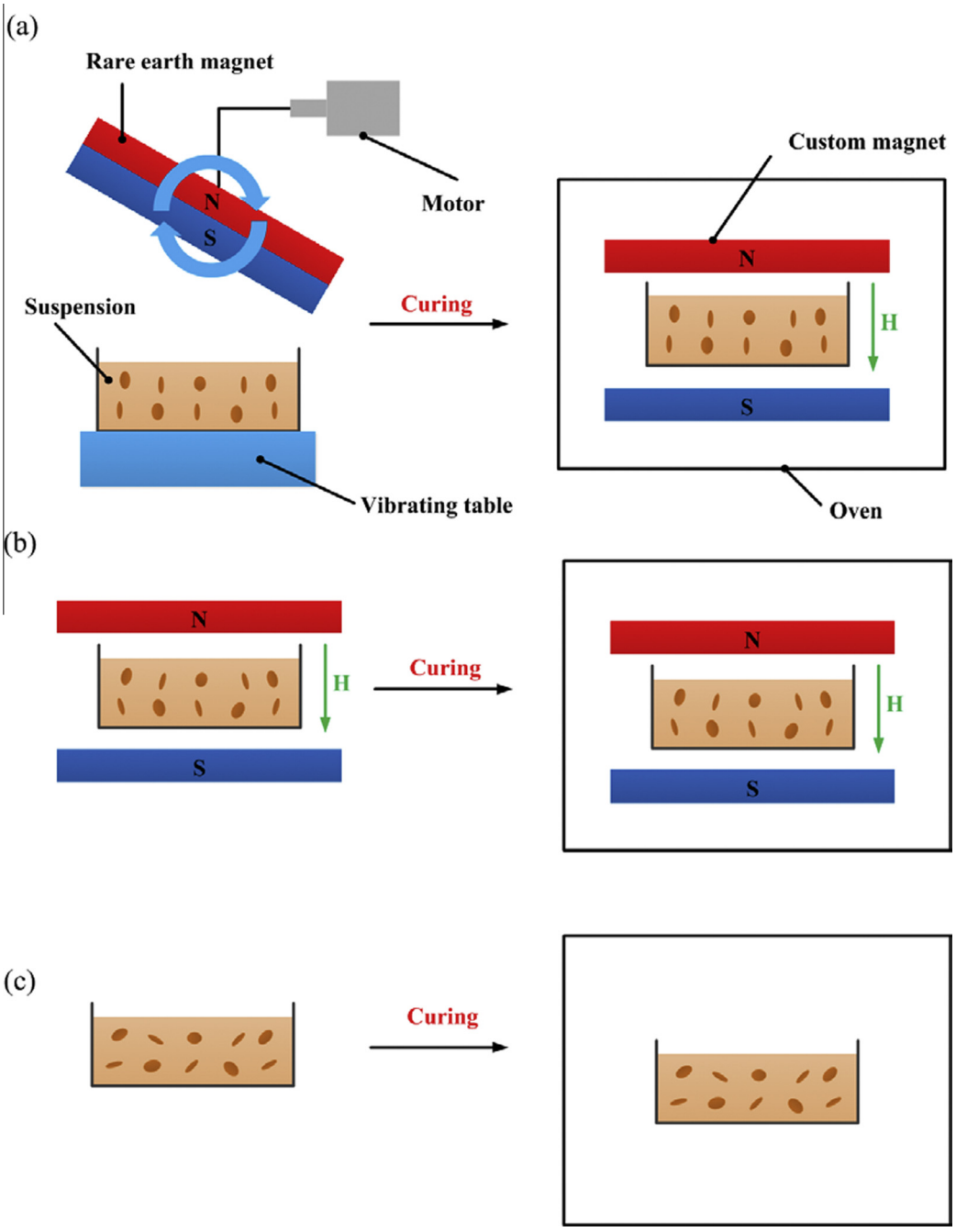

Fig. 2. Description for the preparation of mhBN–resin composites with (a) combined mechanical and magnetic stimuli, (b) magnetic stimuli and (c) no stimuli.

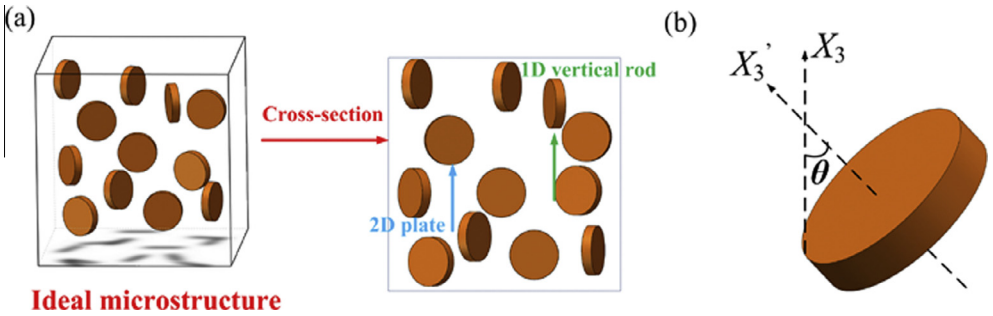

Fig. 3. (a) Ideal microstructure of composites contacting the well-aligned platelets and the representative morphologies of platelets at the cross sectional view. (b) Schematic of a platelet with the angle θ. (For interpretation of the references to colour in this figure legend, the reader is referred to the web version of this article.)

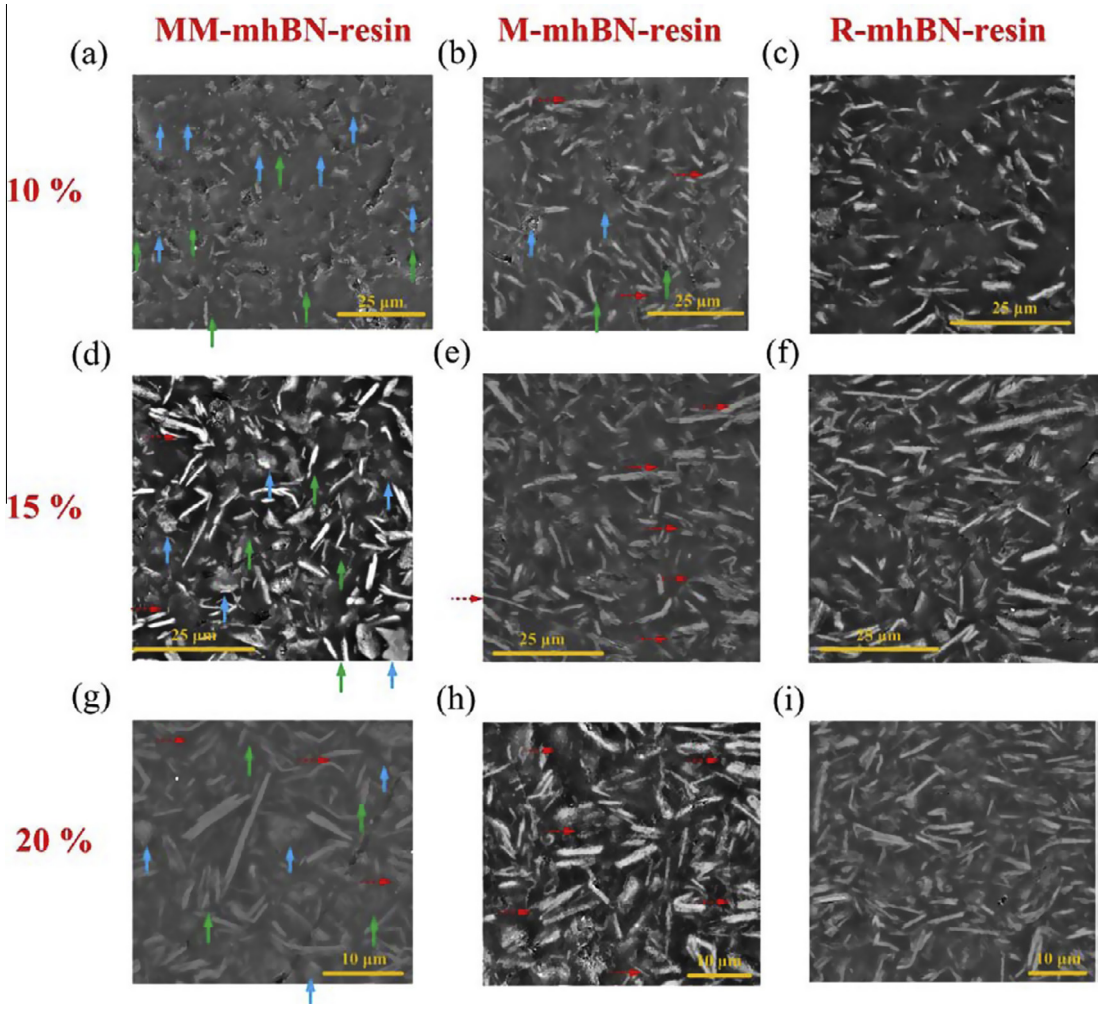

Fig. 4. Cross-sectional SEM images of MM-mhBN–resin composites at *f* of (a) 10%, (d) 15% and (g) 20%, M-mhBN–resin composites at *f* of (b) 10%, (e) 15% and (h) 20%, and R-mhBN–resin composites at *f* of (c) 10%, (f) 15% and (i) 20%. 1D vertical rods and 2D plates are indicated by green and blue arrows, respectively, and the unexpected morphology is indicated by red arrows. (For interpretation of the references to colour in this figure legend, the reader is referred to the web version of this article.)

axis X_3 and the local particle symmetric axis X_3'. When the platelet aligns along the vertical or horizontal direction, θ is equal to 90° or 0°, respectively. The results are represented as a distribution histogram in Fig. 5 and the parameter, *P*, is defined as population-fraction of the platelets to be above 45°. Table 1 summarizes the values of *P* for the MM-mhBN–resin and M-mhBN–resin composites. It is found that in the 10 vol.% MM-mhBN–resin, θ of 95.3% of platelets is greater than 45°, only ~5% of platelets have fallen into the horizontal direction. While, in the M-mhBN–resin with same *f*, *P* decreases to 74.7%. This means that the ratio of in-plane oriented platelets increases. In addition, for the composites at *f* of 15% and 20%, the MM-mhBN–resin also exhibits higher value of *P*.

XRD analysis is carried out to further evaluate the alignment of mhBNs in resin matrix. Fig. 6 gives the XRD patterns for the 10 vol.% MM-mhBN–resin, M-mhBN–resin and R-mhBN–resin composites. The XRD patterns are compared to show their relative alignment degrees. It is observed that the peak intensities are dramatically different for the three composites. As reported previously [15,17], the vertically and horizontally oriented hBNs are responsive for the (100) and (002) peaks, respectively. Thus, we use the ratio of (100) peak intensity to (002) peak intensity (I_{100}/I_{002}) to estimate the degree of vertical alignment of platelets. Table 2 provides the values of I_{100}/I_{002} for the 10 vol.% mhBN–resin composites. It is found that I_{100}/I_{002} of MM-mhBN–resin is more than 6 times and 28 times larger than that of M-mhBN–resin and R-mhBN–resin, respectively. Table 2 also provides the I_{100}/I_{002} values for the composites with higher loading. I_{100}/I_{002} of MM-mhBN–resin is still higher than other two composites with the same *f*. The higher value suggests the larger amount of vertically aligned mhBNs in MM-mhBN–resin.

3.2. Thermal conductivity of mhBN–resin composites

It has been illustrated that the degree of platelets alignment in matrix is greatly different among the composites fabricated with different methods. We intend to investigate the correlation between the degree of alignment and thermal conductivity of composites. Fig. 7a provides the measured through-plane thermal conductivity (k_T) of MM-mhBN–resin, M-mhBN–resin and R-mhBN–resin composites at *f* from 10% to 20%. It can be observed that k_T is also different among the three composites with the same *f*. k_T of MM-mhBN–resin is highest, whereas that of R-mhBN–resin is lowest. The results demonstrate that there is positive correlation between the degree of alignment and thermal conductivity. To future study the correlation, Fig. 7b gives the thermal enhancements of MM-mhBN–resin and M-mhBN–resin referring to R-mhBN–resin, respectively. For the M-mhBN–resin, thermal enhancement is 36% at 10 vol.%, but drops rapidly to 14% and 6% at 15 vol.% and 20 vol.%, respectively. The drop of thermal

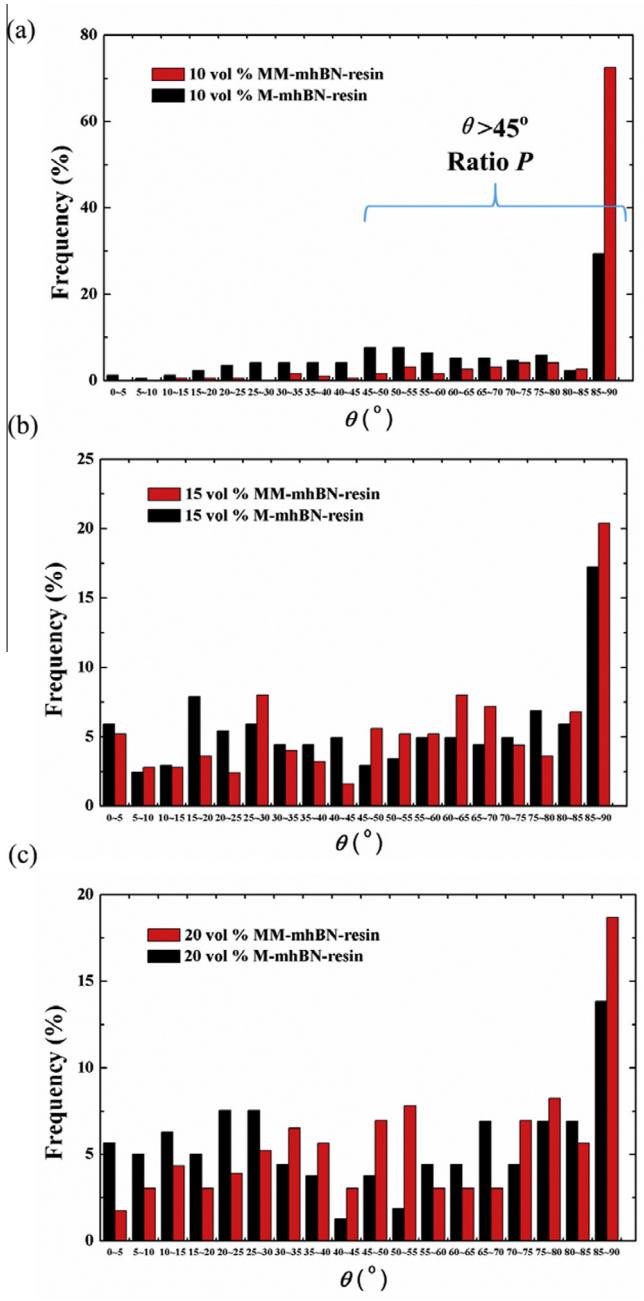

Fig. 5. Angle distribution of mhBNs platelets in MM-mhBN–resin and M-mhBN–resin composites at f of (a)10%, (b) 15% and (c) 20%.

Table 1
Values of P for the MM-mhBN–resin and M-mhBN–resin composites.

Volume fraction (f, %)	P (%)	
	MM-mhBN–resin	M-mhBN–resin
10	95.3	74.7
15	66.4	55.7
20	63.5	53.6

enhancement at high mhBN loadings is due to the decreased degree of mhBN alignment. Thermal enhancement of the MM-mhBN–resin also decreases with the increase of f due to the same reason. However, the MM-mhBN–resin composites achieve greater thermal enhancement. It is found that the thermal enhancement

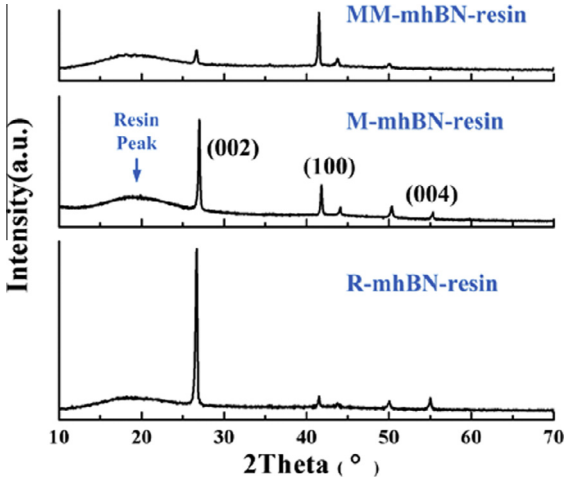

Fig. 6. XRD analysis of 10 vol.% MM-mhBN–resin, M-mhBN–resin and R-mhBN–resin composites.

Table 2
Values of I_{100}/I_{002} for the MM-mhBN–resin, M-mhBN–resin and R-mhBN–resin composites.

Volume fraction (f, %)	I_{100}/I_{002}		
	MM-mhBN	M-mhBN	R-mhBN
10	2.68	0.39	0.10
15	0.15	0.08	0.05
20	0.12	0.07	0.05

reaches to 74% at 10 vol.% and maintains at 20% at higher f. The great thermal enhancement is owing to the formation of conductive networks.

3.3. Theoretical analysis

The modified effective medium approximation (EMA) [24] is applied to analyze the experimental data. It is famous for predicting thermal conductivity of composites containing the platelet-shaped fillers [6,15,17]. It illustrates that thermal conductivity is determined by the intrinsic thermal properties of fillers and matrix, fillers loading, geometries, orientations, and the thermal boundary resistance (R_b) at the filler−matrix interface. In this model, the orientational characteristic of fillers in matrix is presented by the parameter, $\langle\cos^2\theta\rangle$, which is expressed as [24]:

$$\langle\cos^2\theta\rangle = \frac{\int \rho(\theta)\cos^2\theta\sin\theta d\theta}{\int \rho(\theta)\sin\theta d\theta} \quad (2)$$

where θ is the angle which has been schematically shown in Fig. 3b and $\rho(\theta)$ is the distribution function of θ. With the aid of distribution histograms (Fig. 5), $\langle\cos^2\theta\rangle$ of the MM-mhBN–resin and M-mhBN–resin composites can be calculated using the discretization method. For the R-mhBN–resin, the platelets are assumed to be completely randomly oriented in matrix. Thus, $\langle\cos^2\theta\rangle = 1/3$ [24]. Table 3 summarizes the values of $\langle\cos^2\theta\rangle$ for all mhBN–resin composites.

In addition to orientation, R_b is another key parameter governing the thermal transport in composites. R_b arises from the poor mechanical or chemical adherence at the interface and the thermal expansion mismatch [5,6,9,24]. In this study, the additional iron oxide nanoparticles on the hBN surface also results in R_b at the interface. In general, the actual R_b can be extracted by fitting the measured thermal conductivity to model prediction [15,17,25]

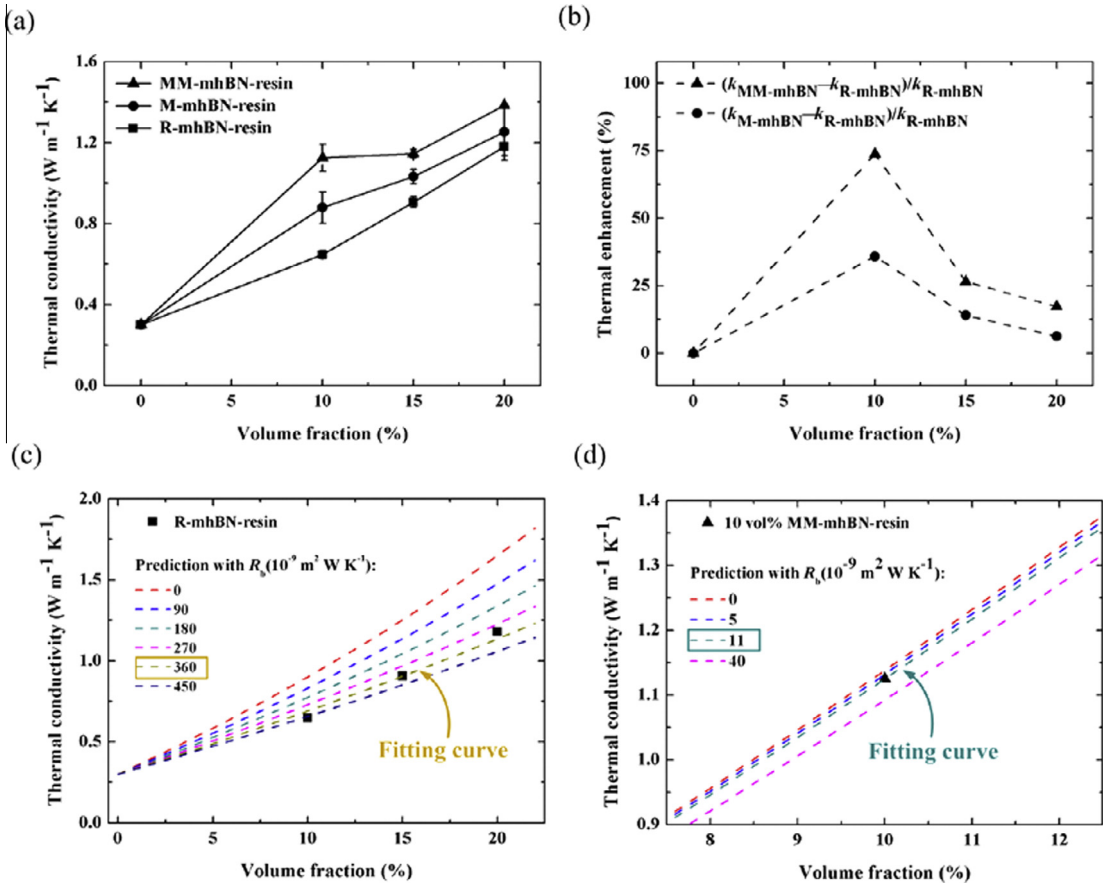

Fig. 7. (a) Thermal conductivities of mhBN–resin composites. (b) Thermal enhancements of MM-mhBN–resin and M-mhBN–resin referring to R-mhBN–resin, respectively. Data fitting to extract R_b of (c) R-mhBN–resin and (d) 10 vol.% MM-mhBN–resin composites. Black dots: measured k_T of composites; Colored dash lines: predicted k_T from effective medium approximation (EMA) with different values of R_b. (For interpretation of the references to colour in this figure legend, the reader is referred to the web version of this article.)

(see details in Appendix B). For R-mhBN–resin composites, Fig. 7c shows the predicted k_T under different values of R_b and the measured k_T of 10, 15 and 20 vol.% composites. R_b is found to be 360×10^{-9} m^2 W K^{-1}. For the MM-mhBN–resin and M-mhBN–resin composites, $\langle\cos^2\theta\rangle$ is different for each composite. Therefore, R_b of each composite is extracted according to its own $\langle\cos^2\theta\rangle$. Fig. 7d shows the predicted k_T of 10 vol.% MM-mhBN–resin under different values of R_b. R_b is fitted to be 11×10^{-9} m^2 W K^{-1}. The way of extracting R_b for other MM-mhBN–resin and M-mhBN–resin composites is the same with that for 10 vol.% MM-mhBN–resin composite. All the fitting results are summarized in Table 3. It is interesting to note that R_b decreases with the reduction of $\langle\cos^2\theta\rangle$, which means that the higher degree of platelets alignment leads to the lower value of R_b. The same results have also been observed in other hBN–polymer interfaces [15,17] and the interfaces with graphite or carbon nanotubes [26–27], which have similar atomic structure to hBN. In addition, theoretical calculation can also explain this point. Prasher [28] theoretically calculated R_b between an anisotropic material and an isotropic substrate. Fig. 8 schematically shows two contact situations. For the anisotropic material, such as hBN, graphite and carbon nanotubes, effective

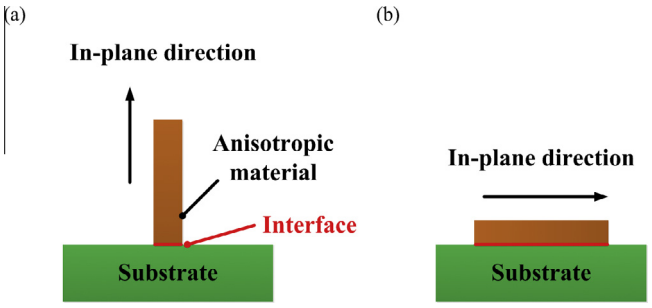

Fig. 8. Schematic showing the two contact situations: (a) vertical contact and (b) horizontal contact.

Table 3
Values of $\langle\cos^2\theta\rangle$ and R_b for the MM-mhBN–resin, M-mhBN–resin and R-mhBN–resin composites.

Volume fraction (f, %)	$\langle\cos^2\theta\rangle$			$R_b \times 10^{-9}$ (m^2 W K^{-1})		
	MM-mhBN	M-mhBN	R-mhBN	MM-mhBN	M-mhBN	R-mhBN
10	0.0530	0.2137	0.3333	11	145	360
15	0.2316	0.2625	0.3333	186	275	360
20	0.2529	0.2724	0.3333	232	317	360

velocity of phonons at the in-plane direction is larger than that at the through-plane direction [28]. Due to the larger phonons velocity at the in-plane direction, R_b for the vertical contact is smaller than that for the horizontal contact [28]. Accordingly, in the mhBN–resin composite, the higher degree of platelets alignment makes R_b reduced.

According to the above analysis, the thermal conductivity of the composites is strongly associated with the degree of platelets alignment. Assembling the platelets into well-ordered structure can greatly enhance the heat transport capability of composites due to the formation of conductive networks and the reduction of R_b.

4. Conclusions

This work report the use of combined mechanical and magnetic stimuli to fabricate the composites containing well-aligned mhBN platelets. The platelets in the resulting composites exhibit a high degree of alignment. Thermal conductivity of the resulting composites were also measured. The results show that thermal conductivity can be greatly enhanced by the platelets alignment. The modified effective medium approximation (EMA) was applied to analyze the experimental data. By fitting the measured thermal conductivity to the EMA prediction, the thermal boundary resistance (R_b) at the mhBN–resin interface was extracted. It is found that the higher degree of platelets alignment results in a lower value of R_b. We can conclude that aligning the platelets can greatly enhance the heat transport capability of composites due to the formation of conductive networks and the reduction of R_b.

Conflict of interest

None declared.

Acknowledgments

This work was supported partly by National Science Foundation of China (51576078, 51376070), and partly by 973 Project of the Ministry of Science and Technology of China (2011CB013105). The authors would like to thank Ms. Luo Huiqian for assistance with the SEM imaging and Mr. Yang Dongwang for assistance with thermal diffusivity measurements.

Appendix A. Calculation of critical frequency

The critical frequency, w_c, is defined as [23]:

$$w_c = \frac{\mu_0 \chi_{ps}^2 H_0^2}{18(F/F_0)\eta(\chi_{ps}+1)}\left[\frac{8(t/2+d)(D/2+d)^2}{tD^2}-1\right] \tag{A.1}$$

$$F/F_0 = \frac{4}{3}\frac{1-(D/t)^2}{(2-(D/t)^2 tS/2)} \tag{A.2}$$

$$S = (4/t)[(D/t)^2-1]^{-1/2}\tan^{-1}\left[((D/t)^2-1)^{1/2}\right] \tag{A.3}$$

where μ_0 is the magnetic permeability of free space, H_0 is the intensity of the magnetic field, D and t are the diameter and thickness of platelet, d is the diameter of iron oxide nanoparticles, η is viscosity of matrix, and χ_{ps} is the magnetic susceptibility of the platelet shell which is estimated from the packing fraction of iron oxide nanoparticles on the platelet shell [23].

To calculate w_c, the parameters are given as follows:

$\mu_0 = 4\pi \times 10^{-7}$ m kg s^{-2} A^{-2}, H_0 = 8000 Gs, D = 5 μm, t = 250 nm, d = 20 nm, η = 0.27 Pa s, χ_{ps} is estimated to be 1.5 [23].

Using Eq. (A.1), w_c is calculated to be 0.3 Hz.

Appendix B. Effective medium approximation for the prediction of composite thermal conductivity and extraction of thermal boundary resistance

B.1. Basic framework

For the composite with particles dispersed in a matrix, the effective through-plane thermal conductivity, k_{33}^*, can be expressed as [24]:

$$k_{33}^* = k_m\frac{1+f[\beta_{11}(1-L_{11})(1-\langle\cos^2\theta\rangle)+\beta_{33}(1-L_{33})\langle\cos^2\theta\rangle]}{1-f[\beta_{11}L_{11}(1-\langle\cos^2\theta\rangle)+\beta_{33}L_{33}\langle\cos^2\theta\rangle]} \tag{B.1}$$

With

$$\beta_{ii} = \frac{k_{ii}^c - k_m}{k_m + L_{ii}(k_{ii}^c - k_m)} \tag{B.2}$$

$$\langle\cos^2\theta\rangle = \frac{\int\rho(\theta)\cos^2\theta\sin\theta d\theta}{\int\rho(\theta)\sin\theta d\theta} \tag{B.3}$$

where 33 and 11 represent through-plane and in-plane direction, respectively; θ is angle between the composite axis X_3 and the local particle symmetric axis X_3'; $\rho(\theta)$ is a distribution function describing the orientation of particles; f is volume fraction of particles; k_{ii}^c is the equivalent thermal conductivity along the ii symmetric axis of the composite unit cell and given by:

$$k_{ii}^c = k_p/(1+\gamma L_{ii}k_p/k_m) \tag{B.4}$$

where k_p and k_m are the thermal conductivities of the particles and matrix, respectively; L_{ii} is the geometrical factor dependent on the particle shape. For the platelet-shaped particle,

$$L_{11} = \frac{p^2}{2(p^2-1)} + \frac{p}{2(1-p^2)^{3/2}}\cos^{-1}p \tag{B.5}$$

$$L_{33} = 1 - 2L_{11} \tag{B.6}$$

$$p = t/D \tag{B.7}$$

where p is the inverse of particle aspect ratio. For platelets, $p < 1$.

$$\gamma = (1+2p)R_b k_m/t \tag{B.8}$$

where R_b is thermal boundary resistance.

B.2. Extraction of R_b for R-mhBN–resin composites

For the R-mhBN–resin composites, the platelets are assumed to be completely randomly oriented in matrix. Thus, $\langle\cos^2\theta\rangle = 1/3$ [24], Eq. (B.1) could be reduced to:

$$k_{33}^* = k_m\frac{3+f[2\beta_{11}(1-L_{11})+\beta_{33}(1-L_{33})]}{3-f[2\beta_{11}L_{11}+\beta_{33}L_{33}]} \tag{B.9}$$

k_m, k_p, D and t are input as known parameter: k_m = 0.3 W m^{-1} K^{-1}, k_p = 390 W m^{-1} K^{-1}, D = 5 μm, t = 250 nm.

Now, R_b is the only unknown parameter in the calculation of k_{33}^*. Fig. 7c gives the predicting results of k_{33}^* under different values of R_b. We assume that R_b is the same for the R-mhBN–resin composites with different f. Thus, R_b can be extracted by fitting their

experimental data to one of the predicting curves. The fitting results are shown in Fig. 7c. R_b is about 360×10^{-9} m^2 W K^{-1}.

B.3. Extraction of R_b for MM-mhBN–resin and M-mhBN–resin composites

As shown in Table 3, $\langle \cos^2\theta \rangle$ is different for each composite. Therefore, R_b of each composite is extracted according to its own $\langle \cos^2\theta \rangle$ and other known parameters. For instance, for the 10 vol.% MM-mhBN–resin composite, the parameters are input as follows:

$\langle \cos^2\theta \rangle = 0.053$, $f = 0.1$, $k_m = 0.3$ W m^{-1} K^{-1}, $k_p = 390$ W m^{-1} K^{-1}, $D = 5$ μm, $t = 250$ nm.

Then, the predicting results of 10 vol.% MM-mhBN–resin under different R_b are obtained with Eq. (B.1) and shown in Fig. 7d. Then, R_b of the composite can be extracted by fitting its experimental result to one of the predicting curves. The fitting result is also given in Fig. 7d. R_b is found to be 11×10^{-9} m^2 W K^{-1}.

The way of extracting R_b for other MM-mhBN–resin and M-mhBN–resin composites is the same with that for 10 vol.% MM-mhBN–resin composite. All the extraction results are summarized in Table 3.

Reference

[1] D. Lu, C.P. Wong, Materials for Advanced Packaging, Springer, New York, 2009.
[2] C.P. Wong, K.S. Moon, Y. Li, Nano-Bio-Electronic, Photonic and MEMS Packaging, Springer, New York, 2010.
[3] S. Liu, X.B. Luo, LED Packaging for Lighting Applications: Design, Manufacturing, and Testing, John Wiley & Sons Press, New York, 2011.
[4] A.L. Moore, L. Shi, Emerging challenges and materials for thermal management of electronics, Mater. Today 17 (4) (2014) 163–174.
[5] R.S. Prasher, J. Shipley, S. Prstic, P. Koning, J.L. Wang, Thermal resistance of particle laden polymeric thermal interface materials, J. Heat Transfer 125 (6) (2003) 1170–1177.
[6] R.S. Prasher, Thermal interface materials: historical perspective, status, and future directions, Proc. IEEE 94 (8) (2006) 1571–1586.
[7] K.C. Otiaba, N.N. Ekere, R.S. Bhatti, S. Mallik, M.O. Alam, E.H. Amalu, Thermal interface materials for automotive electronic control unit: trends, technology and R&D challenges, Microelectron. Reliab. 51 (12) (2011) 2031–2043.
[8] S. Mallik, N. Ekere, C. Best, R. Bhatti, Investigation of thermal management materials for automotive electronic control units, Appl. Therm. Eng. 31 (2–3) (2011) 355–362.
[9] C. Yuan, X.B. Luo, A unit cell approach to compute thermal conductivity of uncured silicone/phosphor composites, Int. J. Heat Mass Transfer 56 (1–2) (2013) 206–211.
[10] E.K. Sichel, R.E. Miller, M.S. Abrahams, C.J. Buiocchi, Heat capacity and thermal conductivity of hexagonal pyrolytic boron nitride, Phys. Rev. B 13 (1976) 4607–4611.
[11] B.H. Xie, X. Huang, G.J. Zhang, High thermal conductive polyvinyl alcohol composites with hexagonal boron nitride microplatelets as fillers, Compos. Sci. Technol. 85 (2013) 98–103.
[12] M. Tanimoto, T. Yamagata, K. Miyata, S. Ando, Anisotropic thermal diffusivity of hexagonal boron nitride-filled polyimide films: effects of filler particle size, aggregation, orientation, and polymer chain rigidity, ACS Appl. Mater. Interfaces 5 (10) (2013) 4374–4382.
[13] W.L. Song, P. Wang, L. Cao, A. Anderson, M.J. Meziani, A.J. Farr, Y.P. Sun, Polymer/boron nitride nanocomposite materials for superior thermal transport performance, Angew. Chem. Int. Ed. 51 (26) (2012) 6498–6501.
[14] Y.W. Han, S.M. Lv, C.X. Hao, F. Ding, Y. Zhang, Thermal conductivity enhancement of BN/silicone composites cured under electric field: stacking of shape, thermal conductivity, and particle packing structure anisotropies, Thermochim. Acta 529 (2012) 68–73.
[15] C. Yuan, B. Duan, L. Li, B. Xie, M.Y. Huang, X.B. Luo, Thermal conductivity of polymer-based composites with magnetic aligned hexagonal boron nitride platelets, ACS Appl. Mater. Interfaces 7 (23) (2015) 13000–13006.
[16] S. Boussaad, Hexagonal boron nitride compositions characterized by interstitial ferromagnetic layers, process for preparing, and composites thereof with organic polymers, US 8277936 B2.
[17] Z.Y. Lin, Y. Liu, S. Raghavan, K.S. Moon, S.K. Sitaraman, C.P. Wong, Magnetic alignment of hexagonal boron nitride platelets in polymer matrix: toward high performance anisotropic polymer composites for electronic encapsulation, ACS Appl. Mater. Interfaces 5 (15) (2013) 7633–7640.
[18] R.M. Erb, R. Libanori, N. Rothfuchs, A.R. Studart, Composites reinforced in three dimensions by using low magnetic fields, Science 335 (6065) (2012) 199–204.
[19] J.S. Olafsen, J.S. Urbach, Clustering, order, and collapse in a driven granular monolayer, Phys. Rev. Lett. 81 (20) (1998) 4369–4372.
[20] J.S. Olafsen, J.S. Urbach, Two-dimensional melting far from equilibrium in a granular monolayer, Phys. Rev. Lett. 95 (9) (2005) 098002.
[21] A.B. Yu, X.Z. An, R.P. Zou, R.Y. Yang, K. Kendall, Self-assembly of particles for densest packing by mechanical vibration, Phys. Rev. Lett. 97 (26) (2006) 265501.
[22] R. Libanori, R.M. Erb, A.R. Studart, Mechanics of platelet-reinforced composites assembled using mechanical and magnetic stimuli, ACS Appl. Mater. Interfaces 5 (21) (2013) 10794–10805.
[23] R.M. Erb, J. Segmehl, M. Charilaou, J.F. Loffler, A.R. Studart, Non-linear alignment dynamics in suspensions of platelets under rotating magnetic fields, Soft Matter 8 (29) (2012) 7604–7609.
[24] C.W. Nan, R. Birringer, D.R. Clarke, H. Gleiter, Effective thermal conductivity of particulate composites with interfacial thermal resistance, J. Appl. Phys. 81 (10) (1997) 6692–6699.
[25] H.Y. Yan, Y.X. Tang, W. Long, Y.F. Li, Enhanced thermal conductivity in polymer composites with aligned graphene nanosheets, J. Mater. Sci. 49 (2014) 5256–5264.
[26] J. Hirotani, T. Ikuta, T. Nishiyama, K. Takahashi, Thermal boundary resistance between the end of an individual carbon nanotube and a Au surface, Nanotechnology 22 (2011) 315702.
[27] A.J. Schmidt, K.C. Collins, A.J. Minnich, G. Chen, Thermal conductance and phonon transmissivity of metal–graphite interfaces, J. Appl. Phys. 107 (2010) 104907.
[28] R.S. Prasher, Thermal boundary resistance and thermal conductivity of multiwalled carbon nanotubes, Phys. Rev. B 77 (2008) 075424.